



Electrochemical Behaviour of AA6061 Alloy in 1M Hydrochloric Acid using Schiff Base Compounds as Corrosion Inhibitors.

Sanaulla Pathapalya Fakrudeen¹, Bheema Raju V².

¹*Department of Engineering Chemistry, HKBK College of Engineering, Nagawara, Bangalore -560045, Karnataka, India.*

²*Department of Chemistry, Dr. Ambedkar Institute of Technology, Mallathahalli, Bangalore – 560056, Karnataka, India*

Received 17 Sept 2012, Revised 16 Nov 2012, Accepted 16 Nov 2012

* Corresponding author. E mail: sanahkbk@gmail.com; Tel 080-25441722.

Abstract

The corrosion inhibition properties of AA6061 Alloy in presence of 1M Hydrochloric Acid by Schiff base compounds namely N, N'-bis (Salicylidene)-1, 4-Diaminobutane (SDB) and N, N'-bis (3-Methoxy Salicylidene)-1, 4 Diaminobutane (MSDB) as corrosion inhibitors were investigated by weight loss, Potentiodynamic polarization(PDP), electrochemical impedance spectroscopy(EIS) and scanning electron microscopy (SEM). Potentiodynamic polarization study revealed that the two Schiff bases acted as mixed type inhibitors. The change in EIS parameters is indicative of adsorption of Schiff bases on aluminium alloys surface leading to formation of protective layer. The weight loss study showed that the inhibition efficiency of these compounds increases with increase in concentration and vary with solution temperature and immersion time. The results obtained from weight loss method, Tafel extrapolation technique and electrochemical impedance spectroscopy were in good agreement. The various thermodynamic parameters were also calculated to investigate the mechanism of corrosion inhibition. The effect of methoxy group on corrosion efficiency was observed from the results obtained between SDB and MSDB. The effectiveness of these inhibitors were in the order of MSDB>SDB. The adsorption of Schiff bases on AA6061 alloy surface in acid obeyed Langmuir adsorption isotherm. The surface characteristics of inhibited and uninhibited alloy samples were investigated by scanning electron microscopy (SEM).

Keywords: Schiff base, Corrosion inhibitors, Aluminium Alloys, Potentiodynamic polarization, EIS.

1. Introduction

Pure aluminium is soft and weak, but it can be alloyed and heat-treated to a broad range of physical and mechanical properties such as tensile strength, yield strength and Brinell hardness. High strength aluminium alloys are considered to be promising structural materials in automobile, defence and aerospace industry because of their excellent combination of low density, high strength and good corrosion resistance.

Aluminium alloys have high resistance to corrosion in many environments due the presence of protective surface film formed rapidly in air or in aqueous solution [1-3]. However, in environments containing aggressive anions, primarily chloride, the protective film gets locally damaged, and corrosive attack takes place. Hydrochloric acid solutions are used for pickling, etching and electrochemical etching in various chemical process industries. It is very important to add a corrosion inhibitor to decrease the rate of dissolution [4, 5]. The organic compounds containing electronegative functional groups (such as N, S, P, O etc) and π -electrons in conjugated double or triple bonds generally exhibit good inhibitive properties by supplying electrons via the pi orbital. The effect of organic compound on the corrosion behaviour of metals or alloys in acidic medium depends on the type of metal and its interaction with the surface of the metal. The inhibition action of organic compounds has been mainly attributed to adsorption of the compound on the surface of the metal which affects the electrochemical reactions involved in the corrosion process of metals or alloys.

The inhibition effect of Schiff base compounds are reported on steel [6-9] copper [10-12] and pure aluminium and its alloys [13-16] in acidic medium. However no substantial work has been carried out on corrosion inhibition of aluminium alloys in acidic medium by Schiff base compounds. Thus, it was thought worthwhile to study the corrosion inhibition behaviour of Schiff base compounds SDB and MSDB on AA6061 Alloy in acid medium.

The present work is aimed at investigating the inhibitive ability of two Schiff base molecules on corrosion of AA6061 alloy in 1M Hydrochloric acid medium. The presence of $-\text{CH}=\text{N}-$ group, an electron cloud on the aromatic ring, the electronegative nitrogen and oxygen atoms in the Schiff base molecules, the Schiff bases should be good corrosion inhibitors [17]. The weight loss, potentiodynamic polarization and electrochemical impedance techniques were employed to study inhibitive effect of two Schiff base molecules at different concentrations. The effect of temperature, immersion time on corrosion behaviour of aluminium alloy was studied in absence and presence of inhibitor at various concentrations by weight loss method. Thermodynamic activation parameters and adsorption isotherm were studied to describe the inhibition mechanism and adsorption behaviour of the Schiff base compounds. For further, confirmation surface morphology of aluminium alloy samples were analyzed by scanning electron microscopic (SEM) technique.

2. Materials and methods

2.1 Aluminium Alloy

The alloy samples were procured from M/S. Fenfe Metallurgical, Bangalore, India. The typical chemical composition of AA6061 alloy in weight percentage is shown in Table 1. The alloy samples were cut into cylindrical test specimens and moulded in cold setting Acrylic resin exposing a surface area of 1.0 cm^2 for electrochemical measurements. For weight loss experiments the cylindrical alloy rods were cut into 24 mm dia x 2mm length-circular cylindrical disc specimens using an abrasive cutting wheel and a 2mm mounting hole at the centre of the specimen was drilled. Before each experiment, the electrodes were abraded with a sequence of emery papers of different grades (600, 800, and 1200), washed with double distilled water, degreased with acetone and dried at 353 K for 30 min in a thermostat electric oven and stored in a moisture-free desiccator prior to use. The corrosive medium selected for this study was 1M hydrochloric acid, which was prepared from analytical grade 37 percent acid concentrated (Merck) in double distilled water.

Table 1: Typical Chemical Composition of AA 6061

Element	Cu	Mg	Si	Fe	Mn	Ti	Cr	Zn	Others	Al
Wt.%	0.15 - 0.40	0.8 - 1.2	0.4 - 0.8	0.7 Max	0.15 Max	0.15 Max	0.04- 0.35	0.25 Max	0.15 Max	Reminder

2.2 Inhibitor.

The Schiff Bases were prepared by the condensation of respective aromatic aldehydes with each of diamines as per the reported procedure [18]. All reagents used were of analytical grade procured from Sigma Aldrich. N,N'-bis(Salicylidene)-1,4-Diaminobutane (SDB) was prepared by slow addition of Salicylaldehyde (2 mmol) in 30 mL methanol over a solution of 1,4-diaminobutane (1mmol) in 30 mL methanol and N,N'-bis(3-MethoxySalicylidene)-1,4-Diaminophenylene (MSDB) by slow addition of Methoxysalicylaldehyde (2 mmol) in 30 mL methanol over a solution of 1,4-diaminobutane (1 mmol) in 30 mL methanol taken in a 250 mL condensation flask. In each case, 2-3drops of acetic acid were added to the mixture of aldehyde and diamine with stirring at constant temperature 298K for 1 hour. Further the mixture was refluxed for 4-5 hours on a water bath, heating occasionally to improve the yield of the product. The reaction mixture was cooled to room temperature overnight and the coloured compound was filtered off and dried. The compounds were recrystallised with ethanol. The product identity was confirmed *via* melting points, Fourier transform infrared spectroscopy (FT-IR) and Proton Nuclear Magnetic Resonance (^1H NMR). The structure, molecular formula, molecular mass, melting points are shown in Table-2.

N,N'-bis(Salicylidene)-1,4-Diaminobutane

IR (KBr cm^{-1}): 3400(OH), 3054(=C-H), 2903(-CH), 1628(C=N).

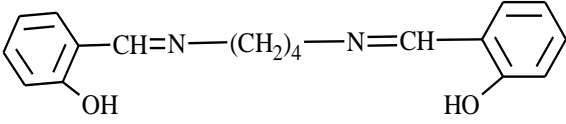
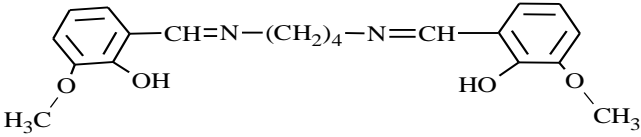
^1H NMR (CDCl_3): δ 1.79-1.82(t, 4H, $-\text{CH}_2\text{CH}_2-$), δ 3.62-3.65(t, 4H, $-\text{CH}_2-\text{N}$) 6.84-7.31 (m, 8H, ArH). 8.34(s, 2H, N=CH), 13.49 (s, 1H, OH),

N,N'-bis(3-Methoxy Salicylidene)-1,4-Diaminobutane

IR (KBr cm^{-1}): 3429(OH), 2996(=C-H), 2932(-CH), 1628(C=N). 1253(-OCH₃).

¹HNMR (CDCl₃): δ 1.80-1.83(t, 4H, -CH₂CH₂-), δ 3.63-3.66(t, 4H, -CH₂-N) δ 3.90(s, 6H, -OCH₃), 6.77-7.2 (m, 6H, ArH). 8.32(s, 2H, N=CH), 14.00 (s, 1H, OH),

Table 2: The structure, molecular formula, molecular mass, melting points

Structure and Name	Molecular Formula	Molecular Mass	Melting Point
 <p>N,N'-bis(Salicylidene)-1,4-Diaminobutane (SDB)</p>	C ₁₈ H ₂₀ N ₂ O ₂	296.36	89°C
 <p>N,N'-bis(3-Methoxy Salicylidene)-1,4-Diaminobutane (MSDB)</p>	C ₂₀ H ₂₄ N ₂ O ₄	356.42	152°C

2.3 Weight loss measurements

Weight loss measurements were performed on aluminium alloys as per ASTM Method [19]. The test specimens were immersed in 100mL 1M hydrochloric acid solution in absence and presence of different concentrations (25,50,75 and 100 ppm) of SDB and MSDB at different temperature ranges (303, 313, 323 and 333 K) in thermostat water bath. The difference in weight for exposed period of 2, 4, 6 and 8 hours was taken as the total weight loss. The weight loss experiments were carried out in triplicate and average values were recorded. The corrosion rate was evaluated as per ASTM Method [19]. The percentage of inhibition efficiency ($\mu_{WL\%}$) and the degree of surface coverage (θ) were calculated using equations (1) and (2):

$$\mu_{WL\%} = \frac{W_o - W_i}{W_o} \times 100 \quad (1)$$

$$\theta = \frac{W_o - W_i}{W_o} \quad (2)$$

Where W_o and W_i are the weight loss values of aluminium alloy sample in the absence and presence of the inhibitor and θ is the degree of surface coverage of the inhibitor.

2.4 Electrochemical measurements.

Potentiodynamic polarization (PDP) and electrochemical impedance spectroscopy (EIS) measurements were performed using CH660c electrochemical workstation. All electrochemical experiments were measured after immersion of alloy specimens for 30 minutes to establish a steady state open circuit potential in absence and presence of inhibitors at 303 K.

Tafel plots were obtained using conventional three electrode Pyrex glass cell with alloy specimen (1cm²) as working electrode (WE), platinum electrode (Pt) as an auxiliary electrode and standard calomel electrode (SCE) as reference electrode. All the values of potential were referred to SCE. Tafel plots were obtained by polarizing the electrode potential automatically from -250 to +250 mV with respect to open circuit potential (OCP) at a scan rate 1mV s⁻¹. The linear Tafel segments of anodic and cathodic curves were extrapolated to corrosion potential (E_{corr}) to obtain corrosion current densities (I_{corr}). The inhibition efficiency was evaluated from the I_{corr} values using the following relationship (3):

$$\mu_p\% = \frac{I_{corr}^0 - I_{corr}}{I_{corr}^0} \times 100 \quad (3)$$

Where, I_{corr}^0 and I_{corr} are values of corrosion current densities in absence and presence of inhibitor respectively.

EIS measurements were carried out in a frequency range from 100 kHz to 0.01 Hz with small amplitude of 10mV peak -to-peak, using AC signal at OCP. The impedance data was analyzed using Nyquist plot and Echem software ZSimpWin version 3.21 was used for data fitting. The inhibition efficiency ($\mu_{\text{Rct}} \%$) was calculated from the charge transfer resistance (R_{ct}) values using following equation (4):

$$\mu_{\text{Rct}} \% = \frac{R_{\text{ct}}^i - R_{\text{ct}}^0}{R_{\text{ct}}^i} \times 100 \quad (4)$$

Where, R_{ct}^0 and R_{ct}^i are the charge transfer resistance in absence and presence of inhibitor, respectively.

2.5 Scanning electron microscopy (SEM).

The surface morphology of the corroded surface in the presence and absence of inhibitors were studied using scanning electron microscope (SEM) [Model No JSM-840A-JEOL]. To understand the surface morphology of the aluminium alloy in the absence and presence of inhibitors, the following cases were examined.

- (i) Polished aluminium alloy specimen.
- (ii) Aluminium alloy specimen dipped in 1M HCl.
- (iii) Aluminium alloy specimen dipped in 1M HCl containing 100 ppm of the Schiff base.

3. Results and discussion

3.1 Potentiodynamic polarisation (PDP)

The polarization measurements of AA6061 alloy specimens were carried out in 1M Hydrochloric acid, in the absence and in the presence of different concentrations (25 -100 ppm) of SDB and MSDB at 303K in order to study the anodic and cathodic reactions. The figure 1(a) and (b) represents potentiodynamic polarisation curves (Tafel plots) of AA6061 alloy in 1M Hydrochloric acid in absence and presence of various concentrations of SDB and MSDB at 303K respectively. The electrochemical parameters i.e. corrosion potential (E_{corr}), corrosion current density (I_{corr}), cathodic and anodic Tafel slopes (b_a and b_c) associated with the polarization measurements of SDB and MSDB are listed in Table.3. The inhibition efficiency ($\mu_p \%$) of inhibitors at different concentrations was calculated from the equation (4). It is observed from the PDP results that, in presence of inhibitors, the curves are shifted to lower current density (I_{corr}) regions and Tafel slopes b_a and b_c values increased with increase in concentration of inhibitors showing the inhibition tendency of SDB and MSDB. The corrosion potential (E_{corr}) values do not show any appreciable shift, which suggest that both inhibitors acted as mixed type but predominantly cathodic inhibitors [20, 21]. This can probably be due to the adsorption of protonated Schiff base molecules on the cathodic and anodic sites.

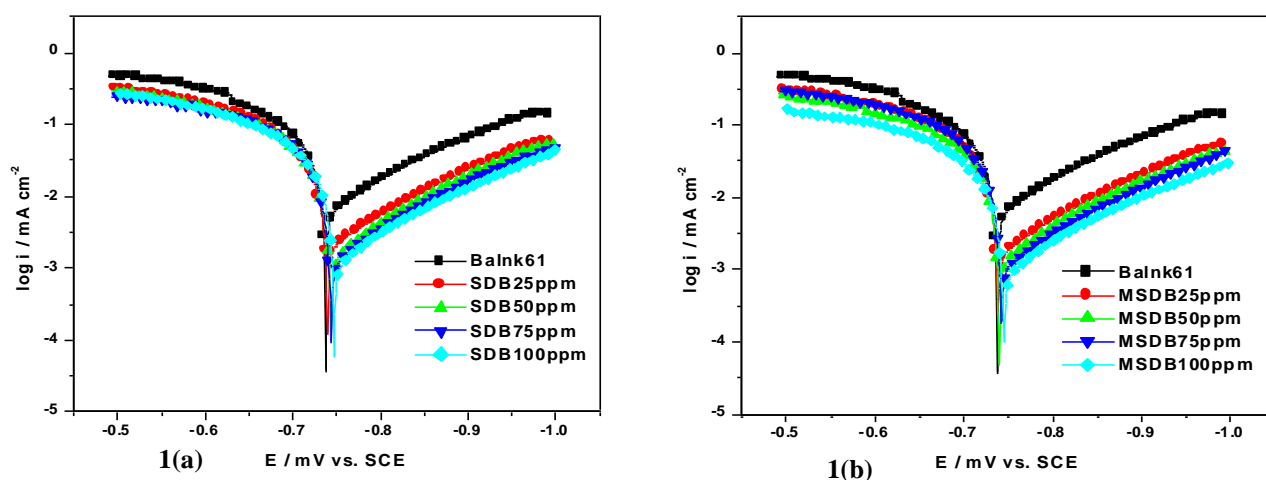


Figure 1: Potentiodynamic polarisation curves (Tafel plots) of AA6061 alloy in 1M Hydrochloric acid in absence and presence of various concentrations of (a) SDB and (b) MSDB at 303K.

Table 3: Potentiodynamic polarisation parameters of AA6061 alloy in 1M Hydrochloric acid in absence and presence of various concentrations of SDB and MSDB at 303K.

Inhibitor	Concentration (ppm)	E_{corr} (mV vs. SCE)	I_{corr} (mA cm ⁻²)	b_c (mV dec ⁻¹)	b_a (mV dec ⁻¹)	$\mu_p\%$
SDB	0	737	9.26	189	68	---
	25	740	3.21	193	81	65.4
	50	743	2.89	196	89	68.7
	75	744	2.66	199	94	71.2
	100	746	2.38	201	98	74.2
MSDB	25	738	2.82	197	87	69.5
	50	740	2.59	198	91	72.0
	75	742	2.26	202	94	75.5
	100	745	1.98	205	96	78.6

3.2 Electrochemical impedance spectroscopy.

The effect of the inhibitor concentration on the impedance behaviour of AA6061 alloy in 1M Hydrochloric acid was studied and Nyquist plots of AA6061 in absence and presence of various concentrations of Schiff bases are given in figure 2 (a) and (b).

It is clear from the figure that the impedance diagrams obtained yield a semicircle shape. This indicates that the corrosion process is mainly controlled by charge transfer. The general shape of the Nyquist plots is similar for all samples of AA 6061 alloy, with a large capacitive loop at higher frequencies and inductive loop at lower frequencies. The similar impedance plots have been reported for the corrosion aluminium and its alloys in hydrochloric acid [22-26].

The Nyquist plot with a depressed semicircle with the centre under the real axis is characteristic property of solid electrode and this kind of phenomenon is known as the dispersing effect [27, 28]. An equivalent circuit fitting of five elements was used to simulate the measured impedance data of AA6061 alloy is depicted in figure 3.

The equivalent circuit includes solution resistance R_s , charge transfer resistance R_{ct} , inductive elements R_L and L . The circuit also consists of constant phase element, CPE (Q) in parallel to the parallel resistors R_{ct} and R_L , and R_L is in series with the inductor L . The impedance spectra for the aluminium alloy in absence and presence of the inhibitors are depressed. The deviation of this kind is referred as frequency dispersion, and has been attributed to inhomogeneous of solid surface of aluminium alloy. Assumption of a simple $R_{ct}-C_{dl}$ is usually a poor approximation especially for systems showing depressed semicircle behaviour due to non – ideal capacitive behaviour of solid electrodes [29]. The capacitor in the equivalent circuit can be replaced by a constant phase element (CPE), which is a frequency dependent element and related to surface roughness. CPE is substituted for the respective capacitor of C_{dl} in order to give a more accurate fit and the impedance function of a CPE has the following equation [30] (5):

$$Z_{\text{CPE}} = \frac{1}{(Y_0 j \omega)^n} \quad (5)$$

Where, Y_0 magnitude of CPE, n is exponent of CPE, and are frequency independent, and ω is the angular frequency for which $-Z''$ reaches its maximum value, n is dependent on the surface morphology : $-1 \leq n \leq 1$. Y_0 and n can be calculated by the equation proved by Mansfeld et al [31].

The double layer capacitance (C_{dl}) can be calculated from the equation (6) [32]:

$$C_{dl} = Y_0 (\omega_{max})^{n-1} \quad (6)$$

Where C_{dl} is the double layer capacitance and ω_{max} is the angular frequency at which $-Z''$ reaches maximum and n is the CPE exponent. The EIS parameters R_s , R_{ct} , ω , CPE, n and C_{dl} are listed in Table-4.

The inhibition efficiency was evaluated by R_{ct} and C_{dl} values of the impedance data, it is shown from Table.(4) that charge transfer resistance (R_{ct}) of inhibited system increased and double layer capacitance

(C_{dl}) decreased with increase in inhibitor concentration. This was due to adsorption of Schiff base molecule on the metal surface, the adsorbed inhibitor blocks either cathodic or anodic reaction or both formation of physical barrier, which reduces metal reactivity. The effect of inhibitor may be due to changes in electric double layer at the interface of solution and metal electrode. The decrease in double layer capacitance (C_{dl}) can be caused by decrease in local dielectric constant and /or increase in the thickness of electric double layer, this suggest that the Schiff base molecules inhibit the aluminium alloy by adsorption at the metal – acid interface[33,34]. It is evident that the inhibition efficiency increases with increase in inhibitor concentration which is in good agreement with the Potentiodynamic polarization results.

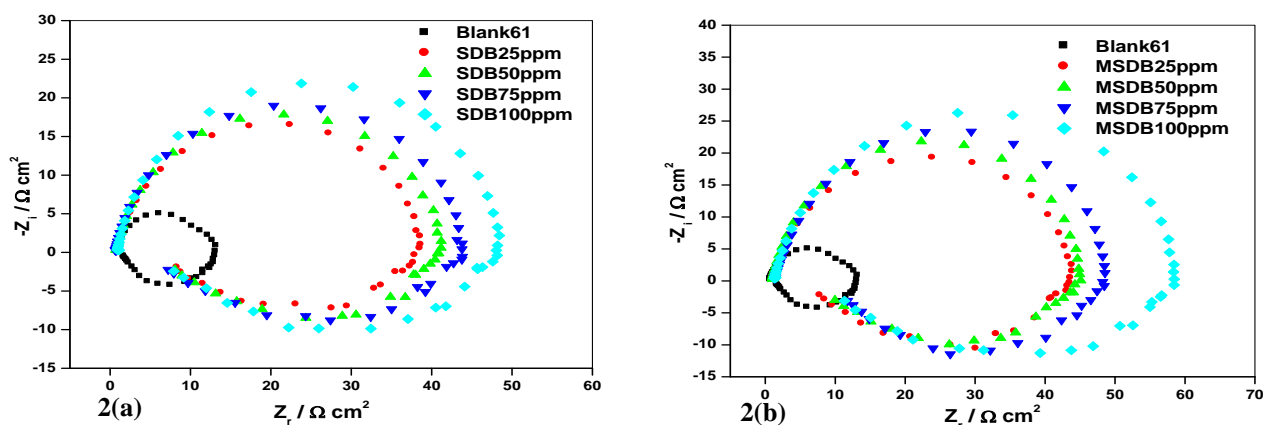


Figure 2: Nyquist plot for AA6061 alloy in 1M Hydrochloric acid in absence and presence of various concentrations of (a) SDB and (b) MSDB at 303K.

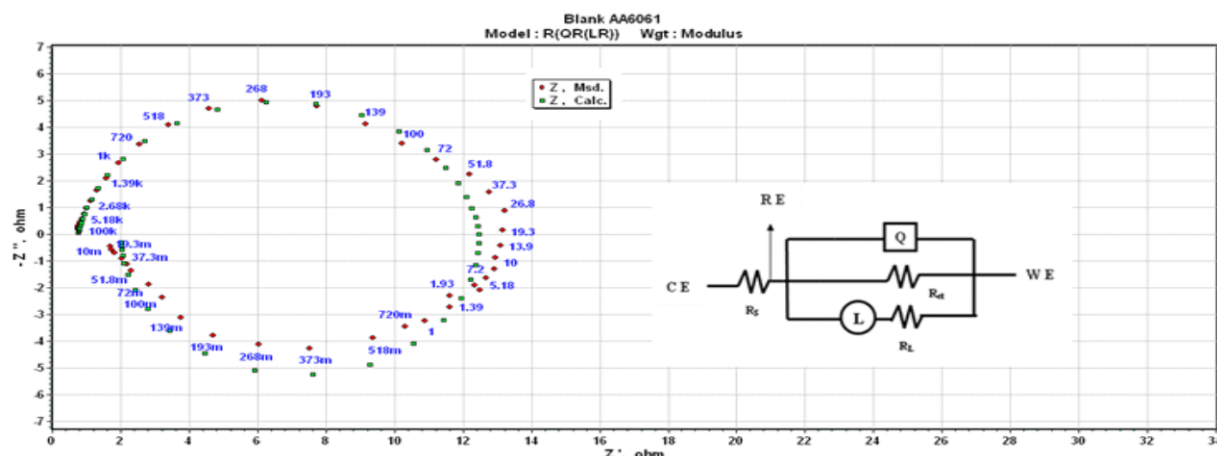


Figure 3: The equivalent circuit model used to fit EIS experimental data.

Table 4: Electrochemical impedance parameters of AA6061 in 1M Hydrochloric acid in absence and presence of various concentrations of (a) SDB and (b) MSDB at 303K

Inhibitor	Concentration (ppm)	R_s ($\Omega \text{ cm}^{-2}$)	R_{ct} ($\Omega \text{ cm}^{-2}$)	ω (Hz)	CPE ($\mu\text{F cm}^{-2}$)	n	C_{dl} ($\mu\text{F cm}^{-2}$)	μ_{Rct} %
SDB	0	1.10	12	4.9	123	0.8905	84.5	---
	25	1.05	35	16	104	0.8790	59.5	65.7
	50	1.12	39	18	68	0.9111	44.7	69.2
	75	1.18	43	19	60	0.9292	42.7	72.0
	100	1.21	45	22	58	0.9311	41.3	73.9
MSDB	25	1.15	41	19	66	0.8986	40.6	70.7
	50	1.19	44	21	63	0.9058	39.8	72.7
	75	1.22	48	23	58	0.9128	37.6	75.0
	100	1.26	55	26	54	0.9157	35.1	78.1

3.3 Weight loss measurements

The experimental data of weight loss (Δw), percentage of inhibition efficiency ($\mu_{WL}\%$), Corrosion Rate (C.R.) in mmpy and degree of Surface Coverage (θ) for AA6061 in 1M HCl in absence and presence of various concentration of SDB and MSDB Schiff bases at 2 hours of exposure time and at 303K are shown in Table. 5.

Table 5: Weight loss parameters for AA6061 in 1M hydrochloric acid in the absence and presence of various concentrations of SDB and MSDB at 2 hours of exposure time and at 303K.

Inhibitor	Conc. /ppm	Δw /mg	$\mu_{WL}\%$	C R / mmpy	θ
SDB	Blank	92.5	-	141.6	-
	25	31.5	66	48.1	0.66
	50	27.8	70	42.5	0.70
	75	25.0	73	38.2	0.73
	100	23.1	75	2.62	0.75
MSDB	25	27.8	70	42.5	0.70
	50	24.1	74	36.8	0.74
	75	21.3	77	32.6	0.77
	100	19.4	79	29.7	0.79

3.3.1 Effect of inhibitor concentration

The variation of inhibition efficiency ($\mu_{WL}\%$) with inhibitor concentration is shown in figure 4(a). Increase in inhibition efficiency at higher concentration of inhibitor may be attributed to larger coverage of metal surface with inhibitor molecules. The maximum inhibition efficiency was achieved at 100 ppm and a further increase in inhibitor concentration caused no appreciable change in performance

3.3.2 Effect of immersion time

The effect of immersion time on inhibition efficiency is shown in figure 4(b). All the tested Schiff bases show a decrease in inhibition efficiency with increase in immersion time from 2 to 8 hours. This indicates desorption of the Schiff Base over a longer test period and may be attributed to various other factors such as formation of less persistent film layer on the metal surface, and increase in cathodic reaction or increase in ferrous ion concentration [35].

3.3.3 Effect of temperature

The influence of temperature on inhibition efficiency of two Schiff bases compounds is shown in figure.4(c). The inhibition efficiency for the two Schiff base compounds decreases with increase in temperature from 303 to 333K. The decrease in inhibition efficiency with rise in temperature may be attributed to desorption of the inhibitor molecules from metal surface at higher temperatures and higher dissolution rates of aluminium at elevated temperatures.

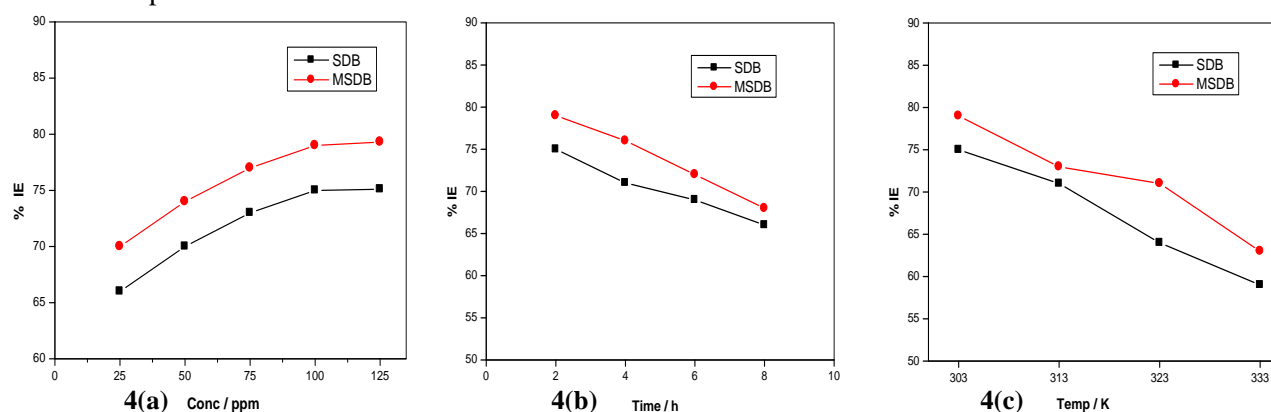


Figure 4: Variation of inhibition efficiency with (a) Inhibitor concentration (b) Exposure time (c) Temperature in 1M Hydrochloric acid for SDB and MSDB.

3.3.4 Thermodynamic activation parameters

Thermodynamic activation parameters are important to study the inhibition mechanism. The activation energy (E_a) is calculated from the logarithm of the corrosion rate in acidic solution is a linear function of $(1/T)$ - Arrhenius equation (7):

$$\log(\text{CR}) = -E_a / 2.303RT + A \quad (7)$$

Where, E_a is the apparent effective activation energy, R is the universal gas constant and A is the Arrhenius pre exponential factor.

Plots of logarithm of corrosion rate obtained by weight loss measurement versus $1/T$ gave straight lines and slope equal to $(-E_a/2.303R)$ as shown in figure 5(a) and 5(b) for SDB and MSDB respectively. The E_a values calculated are listed in Table.6.

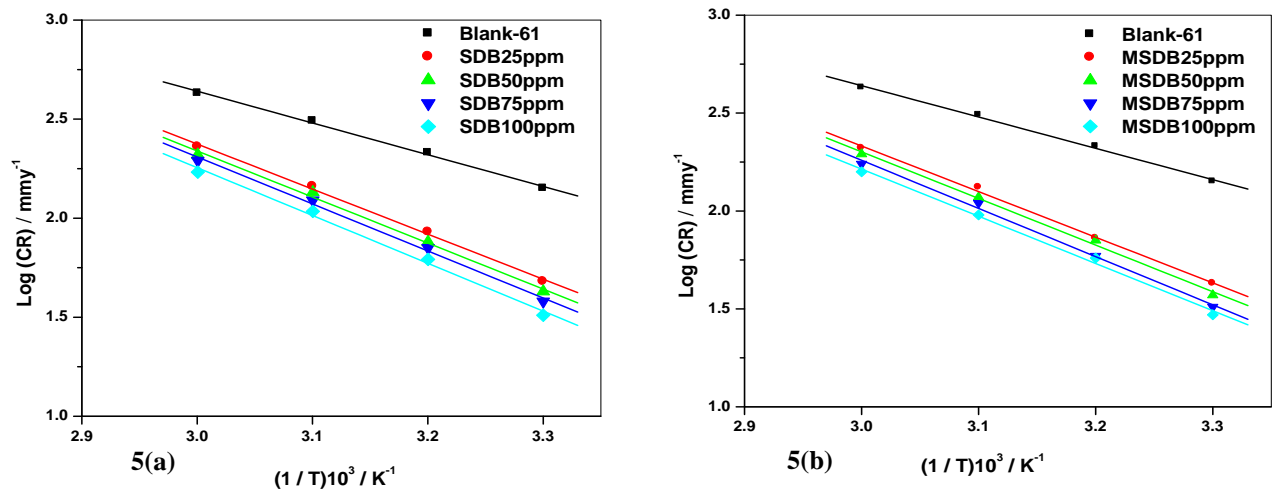


Figure 5: Arrhenius plot of log CR versus $1/T$ in absence and presence of (a) SDB and (b) MSDB

A plot of $\log(\text{CR}/T)$ versus $1/T$ gave a straight line, figure 6(a) and (b) with a slope of $(-\Delta H^*/2.303 R)$ and an intercept of $[(\log(R/Nh) + (\Delta S^*/2.303 R))]$, from which the values of ΔS^* and ΔH^* were calculated. The straight lines were obtained according to transition state equation (8):

$$C R = RT / N h \exp(-\Delta H^* / RT) \exp(\Delta S^* / R) \quad (8)$$

Where, h is the Plank constant, N is the Avogadro number, ΔS^* is entropy of activation and ΔH^* is the enthalpy of activation. The ΔS^* and ΔH^* values calculated are listed in Table. 6

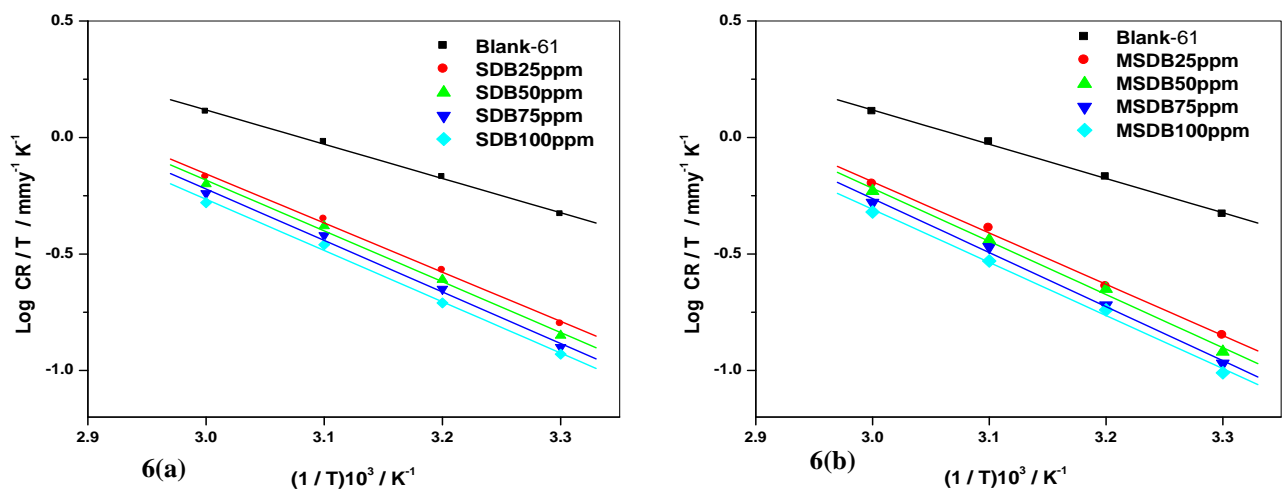


Figure 6: Arrhenius plot of $\log(\text{CR}/T)$ versus $1/T$ in absence and presence of (a) SDB and (b) MSDB

The E_a values of aluminium alloy in 1M Hydrochloric acid in the presence of Schiff base compounds are higher than those in the absence of Schiff bases. The increase in the E_a values, with increasing inhibitor concentration is attributed to physical adsorption of inhibitor molecules on the metal surface [36, 37]. In other words, the adsorption of inhibitor on the electrode surface leads to formation of a physical barrier that reduces the metal dissolution in electrochemical reactions [38]. The inhibition efficiency decreases with increase in temperature which indicates desorption of inhibitor molecules as the temperature increases [39]. The values of enthalpy of activation (ΔH^*) are positive; this indicates that the corrosion process is endothermic and dissolution process of aluminium alloy decreases. The values of entropy of activation (ΔS^*) are higher in the presence of inhibitor than those in the absence of inhibitor. The increase in values of ΔS^* reveals that an increase in randomness occurred on going from reactants to the activated complex [40-42].

Table 6: Thermodynamic parameters of activation of AA6061 in 1M HCl in presence and absence of different concentrations of SDB and MSDB

Inhibitor	Concentration (ppm)	E_a (kJmol ⁻¹)	ΔH^* (kJmol ⁻¹)	ΔS^* (J mol ⁻¹ K ⁻¹)
SDB	0	30.64	28.15	-110.96
	25	42.21	40.40	-79.43
	50	43.55	41.74	-75.92
	75	45.47	42.32	-76.34
	100	46.22	42.13	-74.93
MSDB	25	44.62	42.13	-74.91
	50	45.57	43.66	-70.85
	75	47.10	44.42	-69.39
	100	48.06	45.57	-67.78

3.3.5 Adsorption isotherms

It is generally assumed that the adsorption of the inhibitor at the interface of metal and solution is the first step in the mechanism of inhibition aggressive media. It is also widely acknowledged that adsorption isotherms provide useful insights into the mechanism of corrosion inhibition. The investigated compounds inhibit the corrosion by adsorption at the metal surface. Theoretically, the adsorption process has been regarded as a simple substitution adsorption process, in which an organic molecule in the aqueous phase substitutes the water molecules adsorbed on the metal surface [43]. The surface coverage (θ) value calculated from weight loss data for different concentrations of Schiff bases was used to explain the best adsorption isotherm. The value of surface coverage (θ) was tested graphically for fitting a suitable adsorption isotherm. Attempts were made to fit surface coverage (θ) values of various isotherms including Langmuir, Freundlich and Temkin isotherms. Among three adsorption isotherms obtained, the best fitted isotherm was the Langmuir adsorption isotherm ($C_{(inh)}/\theta$ vs. $C_{(inh)}$) figure 7(a) with a linear regression coefficient values ($R^2=0.9996$) is nearest to one. The Langmuir adsorption isotherm can be expressed by following equation (9):

$$\frac{C_{(inh)}}{\theta} = \frac{1}{K_{(ads)}} + C_{(inh)} \quad (9)$$

Where $C_{(inh)}$ is inhibitor concentration and $K_{(ads)}$ is an equilibrium constant for adsorption and desorption. The $K_{(ads)}$ was calculated from the intercepts of the straight lines on the $C_{(inh)}/\theta$ axis figure 7(a) and standard free energy of adsorption of inhibitor ΔG_{ads}^0 was calculated using the relation (10);

$$\Delta G_{ads}^0 = -RT \ln (55.5 K_{ads}) \quad (10)$$

To calculate heat of adsorption (ΔH_{ads}^0) and entropy of adsorption (ΔS_{ads}^0), $\ln K_{(ads)}$ vs. $1/T$ was plotted as shown in figure 7(b). The straight lines were obtained with a slope equal to $(-\Delta H_{ads}^0/R)$ and intercept equal to $(\Delta S_{ads}^0/R + \ln 1/55.5)$. The values of equilibrium constant ($K_{(ads)}$), Standard free energy of adsorption (ΔG_{ads}^0) enthalpy of adsorption (ΔH_{ads}^0) and entropy of adsorption (ΔS_{ads}^0) are listed in Table.7.

The negative values of standard free of adsorption indicated spontaneous adsorption of Schiff bases on aluminium alloy surface. The calculated standard free energy of adsorption values for the Schiff bases are closer to -40 kJ mole^{-1} and it can be concluded that the adsorption of Schiff bases on the aluminium surface is more chemical than physical one [44]. The sign of enthalpy and entropy of adsorption are positive and is related to substitutional adsorption can be attributed to the increase in the solvent entropy and to a more positive water desorption enthalpy. The increase in entropy is the driving force for the adsorption of the Schiff bases on the aluminium alloy surface.

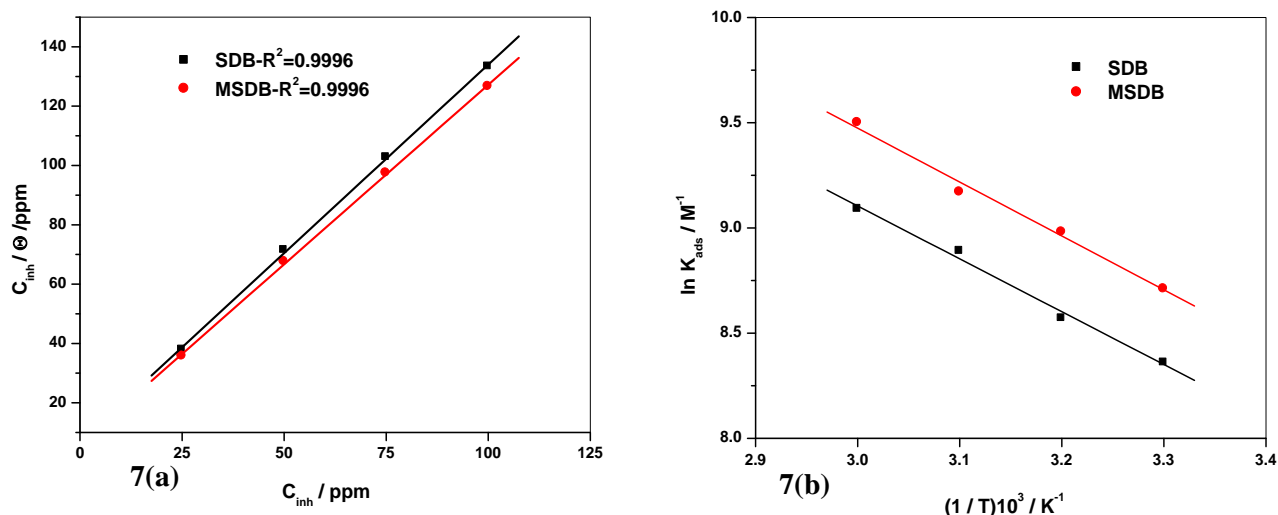


Figure 7: (a) Langmuir adsorption isotherm plot and (b) Heat of adsorption isotherm plot for SDB and MSDB.

Table 7: Thermodynamic parameters for the adsorption of inhibitor in 1M HCl on AA6061 alloy at different temperatures.

Inhibitor	Concentration (ppm)	Temperature (K)	K_{ads} (10^3 M^{-1})	ΔG_{ads}° (kJmol^{-1})	ΔH_{ads}° (kJmol^{-1})	ΔS_{ads}° (Jmol^{-1})
SDB	100	303	8.89	-33	20.9	169
		313	7.26	-34		
		323	5.27	-34		
		333	4.27	-34		
MSDB	100	303	13.4	-34	21.3	176
		313	9.64	-34		
		323	7.93	-35		
		333	6.07	-35		

The adsorption of Schiff base on the aluminium alloy surface can be attributed to adsorption of the organic compounds via phenolic and iminic groups in both cases. Among these two Schiff bases, the chelate effect of MSDB is greater than that of SDB. This is due to the presence of two electron donating groups of $-\text{OCH}_3$ in MSDB structure than SDB. The more efficient adsorption of MSDB is the result of electronegative oxygen atoms present in the MSDB compared to SDB Structure.

3.4 Scanning electron microscope (SEM)

Scanning electron microscopy of the AA6061 sample of inhibited and uninhibited metal samples is presented in Figure 8. The SEM study shows that the inhibited alloy surface is found smoother than the uninhibited surface.

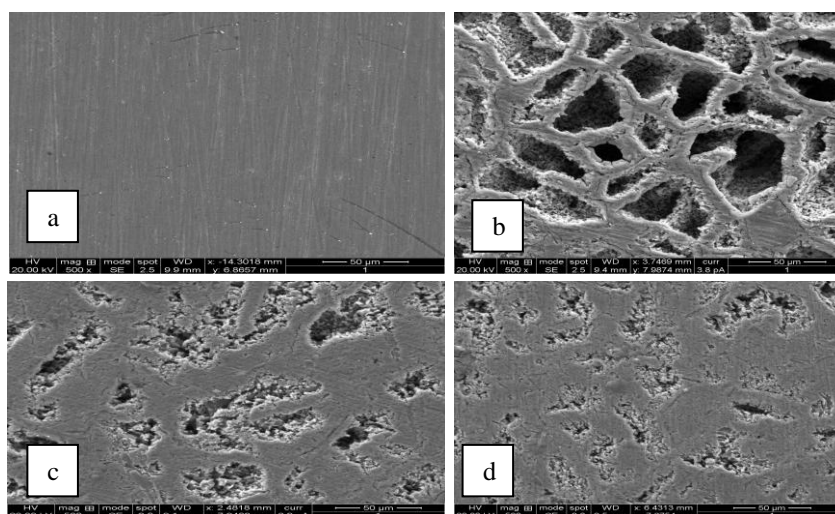


Figure 8: Scanning electron micrographs of (a) Polished AA6061 alloy, (b) After immersion in 1M HCl for 2h, (c) After immersion in 1M HCl for 2h in presence of 100 ppm SDB and (d) After immersion in 1M HCl for 2h in presence of 100 ppm MSDB.

Conclusions

The investigated Schiff bases are good inhibitors for aluminium alloy 6061 in 1M Hydrochloric acid solution. In weight loss studies, the inhibition efficiency ($\mu_{WL}\%$) of the Schiff bases increase with increase in inhibitor concentration, whereas decreases with increase in immersion time and temperature. Potentiodynamic polarisation studies demonstrate the Schiff bases under investigation act as mixed type but predominantly cathodic inhibitors. EIS measurements show that as the inhibitor concentration is increased, the charge transfer resistance increases and double layer capacitance decreases. The inhibition efficiency obtained using weight loss, potentiodynamic polarisation, and EIS studies are in good agreement and in accordance to the order: MSDB > SDB for AA6061 alloy. The adsorptions of Schiff bases on alloy surface in 1M Hydrochloric acid solution are governed by Langmuir adsorption isotherm. Scanning Electron Microscopy (SEM) shows a smoother surface for inhibited alloy samples than uninhibited samples due to formation of protective barrier film.

Acknowledgements

Authors would like to thank for their encouragement to Dr. M.A. Quraishi, Professor of Chemistry, Banaras Hindu University (BHU), Varanasi, India, Dr. D.B. Fakruddin, Professor Emeritus, Siddaganga Institute of Technology, Tumkur, India, Thanks are due to Dr. Syed Abu Sayeed Mohammed, Prof. MN Zulfiqar Ahmed and Mr. Syed Nayazulla of department of Engineering Chemistry, Mrs. Soni. M. EEE department, HKBK College of Engineering, for their contribution during the experimental work.

References

1. C.M. A. Brett, *Corros. Sci.* 33 (1992) 203.
2. Beck TR (1998) *Electrochim Acta* 33:132.
3. Hunkeler F, Frankel GS, Bohni H. *Corrosion* 43:189(1987).
4. G. Schmitt, Br. *Corros. J.* 19, 165 (1984).
5. B. Mernari, H. Elattari, M. Traisnel, F. Bentiss, M. Legrance, *Corros. Sci.* 40, 391, (1998).
6. Ashish Kumar Singh, M. A. Quraishi, *Int. J. Electrochem. Sci.*, 7 (2012) 3222-3241.
7. Fatemeh Baghaei Ravari, Athareh Dadagarinezhad, Iran Shekshoaei, *J. Chi. Chem. Soc.* 55, N° 3 (2010) 328-331.
8. Hahner, G., Woll, Ch., Buck, M., Grunze, M., 1993. *Langmuir*, 9 (1), 955.
9. H. Shorky, M. Yuasa, I. Sekine, R.M. Issa, H.Y. El-Baradie, G.K. Gomma, *Corros. Sci.* 40, 2173 (1998).

10. Fatemeh Baghaei Ravari, Athareh Dadagarinezhad, Iran Shekhshoei, *G.U. Journal of Science*. 22(3);175-182 (2009).
11. Z. Quan, S.H. Chen, Y. Li, X. Cui, *Corros. Sci.* 44, 703 (2002).
12. S.L. Li, Y.G. Wang, S.H. Chen, R. Yu, S.B. Lei, H.Y. Ma, D.X. Liu, *Corros. Sci.* 41, 1769 (1999).
13. A.S. Patel, V.A. Panchal, G.V. Mudaliar, N.K. Singh, *Journal of Saudi Chemical society*, 20June2011.
14. A. S. Patel, V. A. Panchal and N. K. Shah, *PRAJÑĀ - Journal of Pure and Applied Sciences*, Vol. 18: 73 - 75 (2010).
15. T. Sethi, A. Chaturvedi, R. K. Upadhyaya, and S. P. Mathur, *Protection of Metals and Physical Chemistry of Surfaces*, 2009, Vol. 45, No. 4, pp. 466–471.
16. A. S. Fouda, G. Y. Elewady, A. El-Askalany, K. Shalabi, *Zastita Materijala*, 51 (2010) broj 4.
17. Aytac, A., Ozmen, U., Kabasakaloglu, M., 2005. *Mater. Chem. Phys.* 89, 176.
18. John Reglinski , Samantha Morris, Davina E. Stevenson. *Polyhedron* 21 (2002) 2175-2182 .
19. ASTM (2004) Standard practice for Laboratory Immersion Corrosion Testing of Metals G31-72.
20. A. Yurt, S. Ulutas, H. Dal, *Appl. Surf. Sci.* 253 (2006) 919.
21. A. El-Sayed, *Corros. Prev. Control* 43 (1996) 23.
22. M. Metikos-Hukovic, R. Babic, Z. Grubac, *J. Appl. Electrochem.* 28 (1998) 433.
23. C.M.A. Brett, *J. Appl. Electrochem.* 20 (1990) 1000.
24. E.J. Lee, S.I. Pyun, *Corros. Sci.* 37 (1995) 157.
25. K.F. Khaled, M.M. Al-Qahtani, *Mater. Chem. Phys.* 113 (2009) 150.
26. A. Ehteram Noor, *Mater. Chem. Phys.* 114 (2009) 533.
27. T. Pajkossy, *J. Electroanal. Chem.* 364, 111, (1994).
28. W.R. Fawcett, Z. Kovacova, A. Mtheo, C. Foss, *J. Electroanal. Chem.* 326, 91, (1992).
29. R. deLevi, *Electrochem. Acta* 8 (1963) 751.
30. H.J.W. Lenderink, M.V.D. Linden, J.H.W. De Wit, *Electrochim. Acta* 38 (1989) 1993.
31. F. Mansfeld, C.H. Tsai, H. Shih, in: R.S. Munn (Ed.), *Computer Modeling in Corrosion*, ASTM, Philadelphia, PA, 1992, p. 86.
32. C.H. Hsu, F. Mansfeld, *corrosion* 57 (2001) 747.
33. A. K. Singh, M. A. Quraishi, *J. Appl. Electrochem.* 40 (2010) 1293-1306.
34. H. Ashassi-Sorkhabi, D. Seifzadeh, M. G. Hosseini, *Corros. Sci.* 50 (2008) 3363-3370.
35. M.A Quraishi. *Rawat J (2001) Corrosion* 19: 273.
36. A. K. Singh, M. A. Quraishi, *Corros. Sci.* 53 (2011) 1288-1297.
37. H. Ashassi-Sorkhabi, B. Shaabani, D. Seifzadeh, *Appl. Surf. Sci.* 239 (2005) 154.
38. F. Mansfeld, *Corrosion Mechanism*, Marcel Dekkar, New York, 1987, p. 119.
39. Ashish Kumar Singh, M.A. Quraishi, *Corros. Sci.* 52 (2010) 156.
40. E.A. Noor, A.H. Al-Moubaraki, *Mater. Chem. Phys.* 110 (2008) 145.
41. A. Yurt, A. Balaban, S.U. Kandemir, G. Bereket, B. Erk, *Mater. Chem. Phys.* 85(2004) 420.
42. G.E. Badr, *Corros. Sci.* (2009), doi:10.1016/j.corsci.2009.06.017.
43. T. Paskossy, *J. Electroanal. Chem.* 364 (1994) 111.
44. A.Yurt, A. Balaban. S. Ustin Kandemir, G. Bereket. B. Erk, *Materials Chemistry and physics.* 85 (2004) 420-426.